

End-to-end Learning of Image based Lane-Change Decision

Seong-Gyun Jeong, Jiwon Kim, Sujung Kim, and Jaesik Min

Abstract—We propose an image based end-to-end learning framework that helps lane-change decisions for human drivers and autonomous vehicles. The proposed system, Safe Lane-Change Aid Network (SLCAN), trains a deep convolutional neural network to classify the status of adjacent lanes from rear view images acquired by cameras mounted on both sides of the vehicle. Rather than depending on any explicit object detection or tracking scheme, SLCAN reads the whole input image and directly decides whether initiation of the lane-change at the moment is safe or not. We collected and annotated 77,273 rear side view images to train and test SLCAN. Experimental results show that the proposed framework achieves 96.98% classification accuracy although the test images are from unseen roadways. We also visualize the saliency map to understand which part of image SLCAN looks at for correct decisions.

I. INTRODUCTION

Lane-change is a basic driving maneuver that moves the ego-vehicle into the adjacent lane heading the same direction. On the roadway, we often encounter situations to change lanes in order to avoid obstacles, overtake other vehicles, or merge into traffic. Before initiating lane-change, a driver must be aware of his/her surroundings to avoid crash or any other incident. For an inexperienced driver, it is a challenging task to simultaneously perceive traffic of the ego and adjacent lanes. Without concentration, even a skillful driver may cause undesired situations during lane-change.

For safe lane-change decision aids, automakers have developed blind spot detection (BSD) systems¹. To observe the rear side space, automakers equip a vehicle with sensors such as cameras or high frequency radars. The BSD system tracks rear side traffic of the ego-vehicle and warns the driver if the system detects an object entering the blind spot zone.

To make a safe lane-change, autonomous vehicles as well as human drivers generally perform the following steps: 1) *environmental perception* and 2) *maneuver decision making*. For the perception task, researchers attempt to identify driving-relevant objects on the roadway such as vehicles, lanes, and road markings. Specifically, significant progress has been made on computer vision based algorithms for object detection and tracking [1]–[4]. For an in-depth review of computer vision applications for intelligent vehicles, we refer the reader to [5]. In spite of these advances in computer vision algorithms, the use of them may be inadequate for real time applications such as lane-change problem, because

The authors are with autonomous driving team at NAVER LABS Corp., Republic of Korea {seonggyun.jeong, gl.kim, sujung.susanna.kim, jaesik.min}@naverlabs.com

¹The names of technique may vary with the manufacturers, *e.g.*, BLind Spot Information System (BLIS), BLind Spot Monitoring (BSM), BLind Spot Warning (BSW), Side Assist, and *etc.*

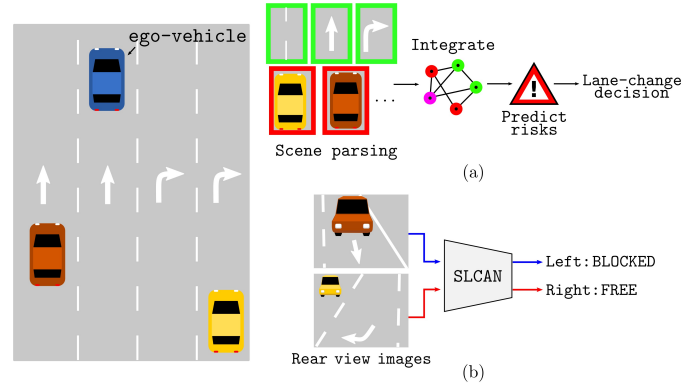


Fig. 1. (a) A typical approach to lane-change decision first detects individual driving-relevant objects with sophisticated perception algorithms. Then, additional steps are needed to integrate the perception results and to compute potential risk of lane-change. (b) The proposed approach trains a DCNN that interprets rear view images and directly renders a lane-change decision.

there are too many object classes that need to be detected and tracked in street scenes, *e.g.*, cars, fence, and trees.

In general, maneuver decision making acts based on the perception results. To predict potential risks for the traffic, the extracted features via perception algorithms are fused by various schemes, *e.g.*, Bayesian networks [6] and fuzzy-related uncertainty representation [7]. In [8], the most relevant features have been investigated with respect to the lane-change intentions in highway scenario. On the other hand, general driver models for lane-change maneuver have been presented, *e.g.*, Foresighted Driver Model (FDM) [9] and Minimizing Overall Braking Induced by Lane changes (MOBIL) [10]. Although the above mentioned approaches allow a safe lane-change, complex procedures are required to interpret the situation with respect to lane-change decision.

Our work is inspired by recent successes that use a Deep Convolutional Neural Network (DCNN) to control autonomous vehicles with end-to-end learning fashion [11], [12]. In [12], the authors trained a DCNN that directly maps an input image into a steer angle value. Chen *et al.* [11] aimed to obtain structured outputs of the driving-relevant objects from an image input rather than directly controlling a car. Our approach lies somewhere between the two algorithms, since our model produces a single output that is used as an aid to the final decision making process. In this work, we expect that a DCNN can learn valid image features so that it classifies the occupancy status of the lanes. Eventually, the proposed framework helps human drivers and autonomous vehicles avoid lane-change crashes.

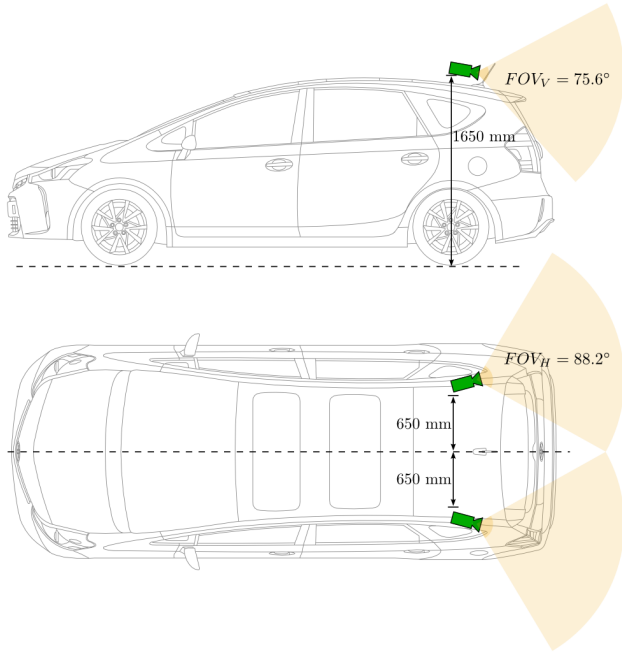


Fig. 2. Our research vehicle senses rear side space with cameras mounted at the both sides.

In this paper, we aim to develop an end-to-end learning framework that assists safe lane-change decision. Instead of object detection or tracking approaches, we formulate an image classification problem that determines the status of adjacent lanes: **BLOCKED** or **FREE** (see Fig. 1). Two cameras with a wide angle lens are installed at the exterior of our research vehicle to acquire rear side view images. To train and test Safe Lane-Change decision Aid Network (SLCAN), we collected and annotated 77,273 images. For an efficient SLCAN training, we annotate the images according to whether the ego-vehicle can move on the corresponding space. The experimental results on driving videos show that SLCAN classifies occupancy status of the lanes with an accuracy over 96.98%.

The main contributions of the paper are

- A novel end-to-end learning system for lane-change is proposed that requires no intermediate stages such as driving-relevant objects perception and risk prediction;
- A new dataset of the rear side view images is collected and annotated to train the proposed system.

The rest of paper is organized as follows. In Section II, we propose an end-to-end learning framework for safe lane-change decision aid. Section III provides extensive experimental results. Finally, we conclude this paper in Section IV.

II. SAFE LANE-CHANGE DECISION AID NETWORK

Our goal is to design a DCNN that can tell whether there is enough room for lane-change at the moment. Unlike the previous approaches [6]–[10], we integrate perception and decision making process into a single image classification process. Intuitively, our approach is more like human driver’s behavior in that a human driver’s decision is based on a glance of very short time instead of systematic analysis of



Fig. 3. Examples of the annotated images for left rear side view: (a) **BLOCKED**, (b) **FREE**, and (c) **UNDEFINED**

surrounding traffic situation. We define the image based lane-change decision problem as follows.

Let $f : I \mapsto \{\text{BLOCKED}, \text{FREE}\} \in \mathbb{A}$ be a function that classifies the given image I onto occupancy status of the corresponding lane. To our best knowledge, we have no dataset for this specific task. We thus create lane-change decision aid dataset which are pairs of image and lane occupancy status $\mathcal{D} = \{(I_k, a_k)\}_{k=1, \dots, K}$, where $a \in \mathbb{A}$ and K denotes the number of images in the dataset. We feed the labelled images to a DCNN in order to learn a function that decides the initiation of the lane-change. For training, softmax loss is employed to quantify the prediction quality compared to groundtruth. With a trained DCNN model, we obtain values which correspond to likelihood probabilities of the current occupancy status for the given image I . Finally we classify the lane status of the input image as follows:

$$f(I) = \underset{a \in \mathbb{A}}{\operatorname{argmax}} P(a | I).$$

A. Collected Data Annotation

SLCAN accepts rear-side view images that are acquired by cameras mounted on the left and right side of the vehicle. To train SLCAN, we need to annotate each acquired image with one of three labels: **BLOCKED**, **FREE**, and **UNDEFINED**. An image is tagged as **BLOCKED** if the adjacent lane is occupied by other vehicles or road structures. On the contrary, an image is tagged as **FREE** if the lane is physically clear enough to initiate lane-change in a few seconds. Here, note that physical clearance overrides the traffic regulations. That is, even in the case that the lane-change is not allowed by a regulation (*e.g.*, changing lane in a tunnel, or even crossing yellow center line), we annotate such images as

FREE if the ego-vehicle can physically move to that lane space. The rationale is that SLCAN is not a final decision maker but an aid module so it should provide as much information as possible to human driver or main controller of the autonomous vehicle. In the case that we cannot determine whether an image is BLOCKED or FREE, we annotate the image as UNDEFINED; for examples, the ego-vehicle is already in the middle of lane-change motion, making a turn at an intersection, or under any other ambiguous situations. To minimize ambiguity in classification, we exclude UNDEFINED labelled images in the training dataset. Fig. 3 shows examples of the annotation results. Moreover, in this work, we use images of typical roadways only; therefore, images of narrow paths or unpaved roads are discarded.

We summarize our annotation criteria as follows:

- BLOCKED if the ego-vehicle cannot physically move to the corresponding space;
- FREE if the ego-vehicle can move to the corresponding space even if such action may violate the traffic regulations;
- UNDEFINED for an ambiguous situation and any other unusual scenes.

A human driver has his/her own decision rule to draw a function $f(\cdot)$ based on individual driving technique and experience. To construct reliable groundtruth $g(\cdot)$, for a given image, we accept the annotation result when all annotation workers agree on; otherwise, the image is tagged as UNDEFINED. More formally,

$$g(I) = \bigwedge_{n=1}^N f_n(I), \quad (1)$$

where $f_n(I)$ denotes the annotated image by n -th worker and \bigwedge is defined as

$$a \wedge b = \begin{cases} \text{BLOCKED}, & \text{if } a \text{ and } b \text{ are both BLOCKED} \\ \text{FREE}, & \text{if } a \text{ and } b \text{ are both FREE} \\ \text{UNDEFINED}, & \text{otherwise.} \end{cases}$$

For all images, at least three workers annotate with respect to the lane status.

B. Network Architecture

We use the VGG 16-layer architecture [13], with the original 1000-way final classification layer replaced by a 2-way classifier. We take the model pre-trained on ILSVRC 2012 dataset [14] and fine-tune it with the dataset we collected to classify the rear view image into two classes: BLOCKED and FREE. In the following section, we give a detailed description of the experiment setup and training procedure.

III. EXPERIMENTS

A. Data Description

We mounted and synchronized two Point Grey Blackfly cameras on the left and right rooftop of the vehicle so that both cameras sense each rear side view space. The camera has 88.2 degrees horizontal and 75.6 degrees vertical field

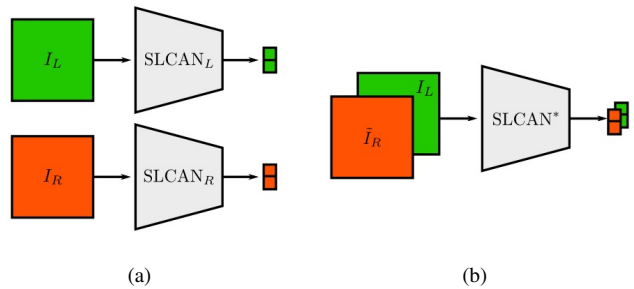


Fig. 4. Illustration of SLCAN architecture configurations: (a) two independent networks that separately train left rear view image I_L and right rear view image I_R , and (b) unified single network that takes left rear view image I_L and flipped right rear view image \bar{I}_R . When deployed on a GPU, configuration of (b) can process two input images in parallel, we save memory space without additional processing time.

TABLE I
DATA CONFIGURATION AND CLASSIFICATION RESULTS^a

Exp.	Model	Accuracy	Dataset			
			BLOCKED	FREE	Total	
E1	SLCAN _L	99.77%	Training	18,390	15,913	34,303
		@Val	Validation	2,043	1,768	3,811
			Test	-	-	-
	SLCAN _R	99.70%	Training	20,512	14,732	35,244
		@Val	Validation	2,279	1,636	3,915
			Test	-	-	-
E2	SLCAN*	99.90%	Training	38,902	30,645	69,547
		@Val	Validation	4,322	3,404	7,726
			Test	-	-	-
E3	SLCAN*	96.98%	Training	34,092	27,284	61,376
		@Test	Validation	3,787	3,031	6,818
			Test	5,345	3,734	9,079

^aIn all cases, the networks were trained up to 5000 epochs.

of view (FOV) with lens of 3.5 mm focal length. Images of 1280×1024 pixel resolution are acquired at the rate of 10 frames per second.

We drove our research vehicle on highway and urban roadway to acquire various scenes and collected a total of 100,088 images (50,044 pairs of left and right images). The images of the dataset consist of various road types (highway, intersection, merge, fork, tunnel, and *etc.*), traffic conditions (from free flow to congestion), types of vehicles (car, truck, bus, van, motorcycle, and *etc.*), and on-road objects and markings (barrier, curb, fence, cone, crosswalk, no stopping zone, and *etc.*).

After annotation work, we set aside all images tagged as UNDEFINED and finally have 38,114 left rear view images (20,433 BLOCKED and 17,681 FREE) and 39,159 right rear view images (22,791 BLOCKED and 16,368 FREE).

B. Configurations

We conducted the following three experiments with different network setups and dataset splits:

E1. Two independent networks for left and right rear view

First, we separately trained two DCNNs for left and right view images, as shown in Fig. 4 (a). Since the two camera views are not symmetric due to the road configuration (*e.g.*, centerline is always observed in the

left rear view images), we supposed that each rear view would need to learn its own model. We split the dataset into 90% training set and 10% validation set (see Table I).

E2. Single network for both cameras

As depicted in Fig. 4 (b), we also trained a unified network for both rear view images, where right view images are horizontally flipped to match left rear view. Training and validation sets were formed by combining the corresponding dataset from both rear view images. The advantage of using a single network is that it can simultaneously process left rear image and flipped right rear image in a batch on a GPU. It requires no additional processing time while only half of the memory space is used comparing to two independent networks architecture.

E3. Single network for both cameras, trained on highway images and tested on urban road images

To see how well our model generalizes to datasets outside the training set, we also experimented training the single network model on highway portion of the dataset and testing it on urban road portion of the dataset. The number of samples for each dataset is given in Table I.

C. Training

Unlike images in general image classification task such as ImageNet, pixels in our road view images have unequal influence on the classification results depending on their location. For example, pixels near leftmost column in left camera view corresponds to the ego-lane and thus can be ignored, while those near rightmost column must not be discarded by cropping as in ImageNet training because it can contain the tail end of the vehicle in an adjacent lane. To preserve such spatial variance of our data, we resize the input images to 256×256 , then a 224×224 patch is cropped at fixed horizontal offset (32 pixels for left camera, 0 pixels for right camera), and random vertical offset (at training time) or vertical center (at test time). For the same reason, we also omit random horizontal flip which is normally employed for data augmentation purpose. For the single network experiments, images from right camera are horizontally flipped. Please see Fig. 5 for an illustration.

For all experiments, we fine-tuned the ImageNet-pretrained VGG-16 network with a minibatch size of 64 and learning rate of 0.001 until convergence. We used Caffe [15] to implement the experiments.

D. Results

We found that a single network trained with left rear view images and horizontally flipped right rear view images performs just as well as networks separately trained for each rear view image. As shown in Table I, we obtained nearly identical validation accuracies for both approaches. Some examples of correct and incorrect classification are shown in Fig. 6. Incorrectly classified samples include borderline cases with adjacent lane vehicle appearing very small at

a far distance, and frame captured under uneven lighting condition.

In Experiment 3, the accuracy slightly decreased by $\sim 3\%$. As shown in Fig. 7, the model is able to correctly classify images containing some obstacles unseen in the training data such as fences or motorcycle, but makes wrong prediction for unseen road markings or large vehicles like a trailer. Still, it performs very well in general, indicating that our model successfully generalizes to unfamiliar scenes.

In Fig. 8, we show saliency maps [16] that visualize which part of the input image influences the classification results the most, by analyzing the magnitude of pixelwise gradients obtained by back-propagation. We can see that the network focuses on obstacles for BLOCKED images, and the road surface of the adjacent lane for FREE images.

To verify whether our model performs reliably over time, we examined the probability of $P(\text{BLOCKED}|I_L(t))$ on a streaming video containing both free and blocked situations (see Fig. 9). In the video, the left lane is free at first and then blocked by stationary obstacles, *e.g.*, trees and curb (orange colored areas on the graph) and freed again, and finally blocked by passing a car (red colored areas). The graph shows that, in most cases, SLCAN's response (blue curve) exactly matches human annotations. The apparent mismatches, right before (d) and right after (f), mostly correspond to the sections annotated as UNDEFINED label, where human annotation workers do not agree unanimously. Moreover, it rarely shows fluctuation without the use of temporal information.

Also, we tested the Experiment 3 model on streaming video including UNDEFINED labeled images, where the images are taken at lane-change motion, roads without lane markings, unusual road markings such as crosswalk or intersection. We found that our model mostly makes correct prediction regarding the occupancy status of adjacent space for such images. We provide video results².

The trained networks can process ~ 94 frames per second on a PC equipped with an NVIDIA GTX 1080 GPU, making it suitable for real-time processing on a consumer-level PC, and even for running on an embedded device at a decent speed.

IV. CONCLUSIONS AND FUTURE WORK

A novel image based end-to-end decision system for safe lane-change has been presented. We showed that even without intermediate steps such as object detection and tracking, direct decision from image pixels achieves an acceptable performance in terms of accuracy (96.98 %) and speed (94 fps). We also showed that, without performance degradation, we can handle left rear view images and flipped right rear view images with a single DCNN instead of handling them with separate DCNNs. The power of generalization is demonstrated by additional experiment where the DCNN trained with images of one type of road (highway) turns out to be able to correctly classify images of another type of

²<https://github.com/jsgyun/SLCAN>



Fig. 5. Illustration of resizing and cropping process for SLCAN input

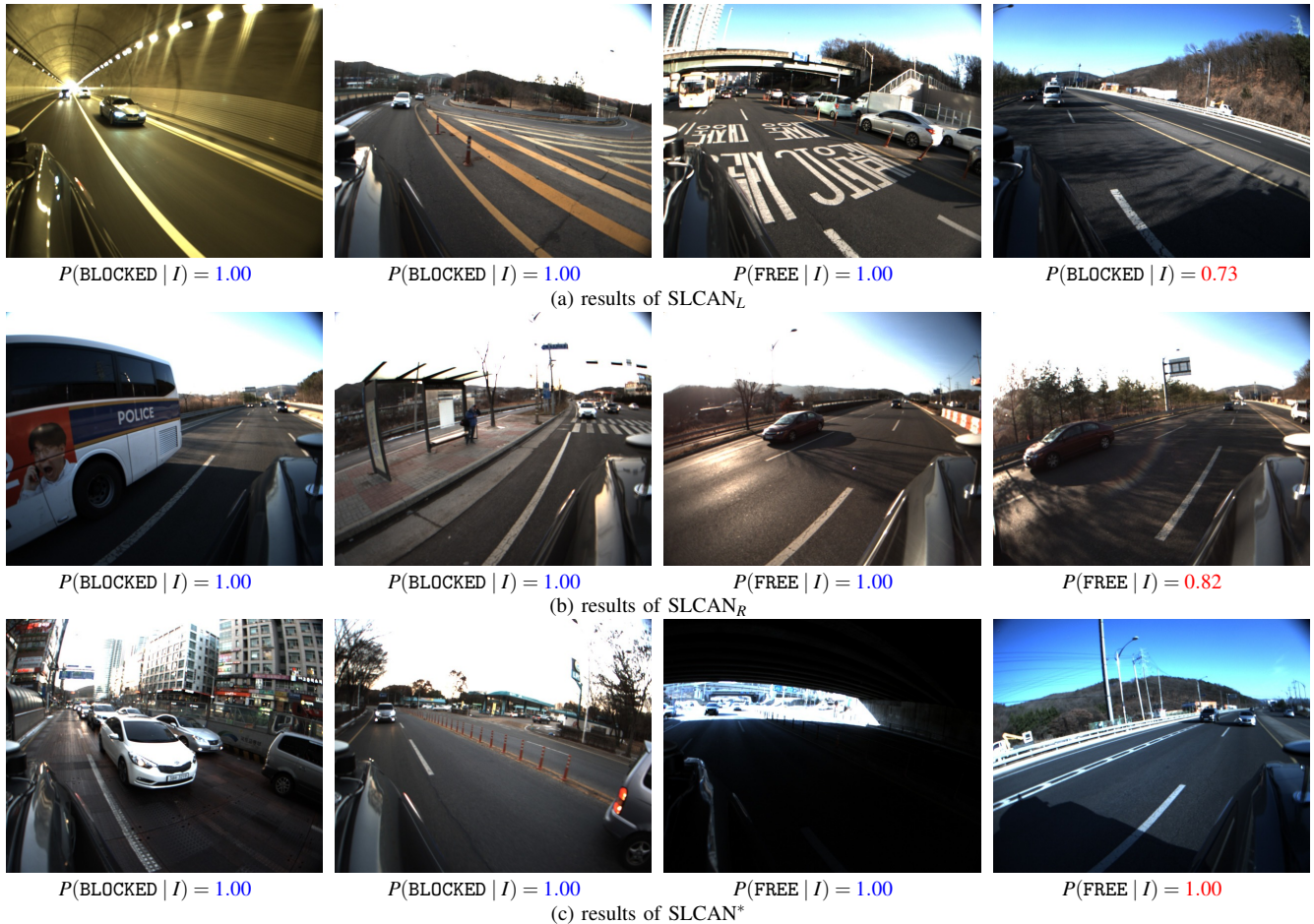


Fig. 6. Experimental results for SLCAN_L, SLCAN_R, and SLCAN*. Colored numbers indicate the probability value returned by DCNN, where blue and red colors denote correct and incorrect classification, respectively. Most of the incorrect classifications (on the rightmost column) actually correspond to situations that are ambiguous or difficult even for humans. (a) The shadows cast by a truck and trees lead to misclassification. (b) The vehicle on the right lane is too far behind to precisely determine the occupancy status of the lane. (c) A vehicle is merging into the right lane.

road (urban roadway). Also, we visualized where SLCAN focuses on in an image to make a decision, which shows that SLCAN behaves like human drivers.

Our future work will be directed towards better generalization and reliability of current method. For generalization, we need to expand the current small and restricted dataset to a larger one that covers various road conditions such as night time scenes, road types, and adverse weather condition. To get more reliable lane-change decision, we would exploit temporal information across consecutive frames since an approaching vehicle at a distance may or may not be a threat depending on the relative speed of that vehicle. To handle this, we plan to design an advanced RNN-based SLCAN that feeds on several consecutive image inputs and returns more

reliable decision.

ACKNOWLEDGEMENT

The authors thank Jongyoon Peck, Jiyoung Jung, Jinhan Lee, Kisung Kim, Namil Kim, Sunwook Choi, and Sungjun Choi from NAVER LABS Corp. for fruitful discussions on SLCAN dataset collection and annotation works.

REFERENCES

- [1] W. Liu, D. Anguelov, D. Erhan, C. Szegedy, S. Reed, C.-Y. Fu, and A. C. Berg, "SSD: Single shot multibox detector," in *European Conference on Computer Vision*, 2016.
- [2] J. Dai, Y. Li, K. He, and J. Sun, "R-FCN: Object detection via region-based fully convolutional networks," in *Neural Information Processing Systems*, 2016.



Fig. 7. Experimental results of correct and incorrect classification with SLCAN*, where the test images are new to the system. (a)–(b): Images with fences and motorcycle, which do not appear in training data, are correctly classified. (c)–(d): SLCAN* is confused to classify `BLOCKED` status with unknown road markings and trailer. Note that the overall classification accuracy is 96.98% and misclassification of this kind is very scarce.

- [3] S. Ren, K. He, R. Girshick, and J. Sun, “Faster R-CNN: Towards real-time object detection with region proposal networks,” in *Neural Information Processing Systems*, 2015.
- [4] Z. Kalal, K. Mikolajczyk, and J. Matas, “Tracking-learning-detection,” *IEEE Transactions on Pattern Analysis and Machine Intelligence*, vol. 34, no. 7, pp. 1409–1422, 2010.
- [5] S. Sivaraman and M. M. Triverdi, “Looking at vehicle on the road: A survey of vision-based vehicle detection, tracking, and behavior analysis,” *IEEE Transactions on Intelligent Transportation Systems*, vol. 14, no. 4, pp. 1773–1795, 2013.
- [6] R. Schubert, K. Schulze, and G. Wanielik, “Situation assessment for automatic lane-change maneuvers,” *IEEE Transactions on Intelligent Transportation Systems*, vol. 11, no. 3, pp. 607–616, 2010.
- [7] M. Pellkofer and E. D. Dickmanns, “Behavior decision in autonomous vehicles,” in *Proceedings of IEEE Intelligent Vehicles Symposium*, 2002.
- [8] J. Schlechtriemen, A. Wedel, J. Hillenbrand, G. Breuel, and K.-D. Kuhnert, “A lane change detection approach using feature ranking with maximized predictive power,” in *Proceedings of IEEE Intelligent Vehicles Symposium*, 2014.
- [9] F. Damerow, B. Flade, and J. Eggert, “Extensions for the foresighted driver model: tactical lane change, overtaking and continuous lateral control,” in *Proceedings of IEEE Intelligent Vehicles Symposium*, 2016.
- [10] A. Kesting, M. Treiber, and D. Helbing, “General lane-changing model mobil for car-following models,” *Journal of the Transportation Research Board*, 1999.
- [11] C. Chen, A. Seff, A. Kornhauser, and J. Xiao, “DeepDriving: Learning affordance for direct perception in autonomous driving,” in *Proceedings of IEEE International Conference on Computer Vision*, 2015.
- [12] M. Bojarski, D. D. Testa, D. Dworakowski, B. Firner, B. Flepp, P. Goyal, L. D. Jackel, M. Monfort, U. Muller, J. Zhang, X. Zhang, J. Zhao, and K. Zieba, “End to end learning for self-driving cars,” *CoRR*, vol. abs/1604.07316, 2016.
- [13] K. Simonyan and A. Zisserman, “Very deep convolutional networks for large-scale image recognition,” *CoRR*, vol. abs/1409.1556, 2014.
- [14] J. Deng, W. Dong, R. Socher, L.-J. Li, K. Li, and L. Fei-Fei, “ImageNet: a large-scale hierarchical image database,” in *Proceedings of IEEE Computer Vision and Pattern Recognition*, 2009.
- [15] Y. Jia, E. Shelhamer, J. Donahue, S. Karayev, J. Long, R. B. Girshick, S. Guadarrama, and T. Darrell, “Caffe: Convolutional architecture for fast feature embedding,” *CoRR*, vol. abs/1408.5093, 2014.
- [16] K. Simonyan, A. Vedaldi, and A. Zisserman, “Deep inside convolutional networks: Visualising image classification models and saliency maps,” *CoRR*, vol. abs/1312.6034, 2013.

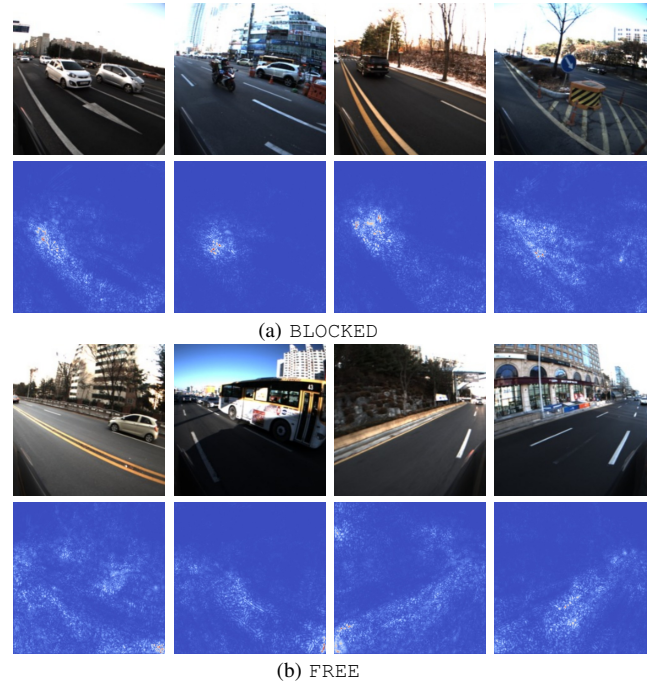


Fig. 8. Saliency maps [13] that show where on the image SLCAN focuses on when it classifies an image. It is apparent that SLCAN focuses on blocking obstacles when they exist and on the road surface when the lane is free.

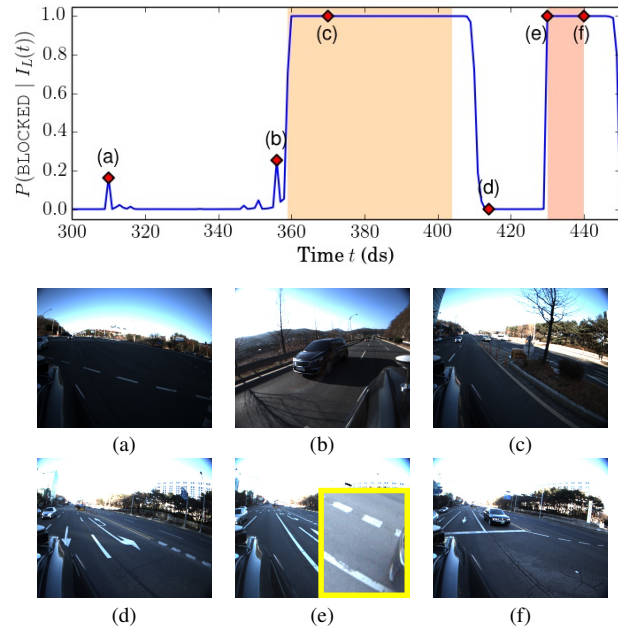


Fig. 9. Comparison of SLCAN’s probabilistic responses with groundtruth annotations on a streaming video. Overall, SLCAN’s response (blue curve) exactly matches human annotations. The apparent mismatches right before (d) and right after (f) mostly correspond to the sections where human annotation workers do not agree unanimously. As can be seen in the magnified image of (e), our model can even detect the tail of a car on the left lane, which is barely visible, and correctly classify it as `BLOCKED`. The graph rarely shows fluctuation without the use of temporal information.